Predicting tropical tree mortality with leaf spectroscopy

Authors: Christopher E. Doughty*[1], Alexander W. Cheesman[2,3], Terhi Riutta[4,5,6], Eleanor Thomson[4], Alexander Shenkin[4], Andrew T. Nottingham[7,8], Walter Huaraca Huasco[4], Noreen Majalap[9], Yit Arn Teh[10], Patrick Meir[11,8], Yadvinder Malhi[4]

Affiliations:

[1]*School of Informatics, Computing, and Cyber Systems, Northern Arizona University, Flagstaff, AZ. 86011, USA*

2 College of Life and Environmental Sciences, University of Exeter, Exeter, Devon EX4 4QF, United Kingdom

3 College of Science & Engineering, James Cook University, Cairns, Queensland 4870, Australia

4 Environmental Change Institute, School of Geography and the Environment, University of Oxford, Oxford OX1 3QY, United Kingdom

5 The Royal Society South East Asia Rainforest Research Partnership, Danum Valley Field Centre, PO Box 60282, 91112 Lahad Datu, Sabah, Malaysia

6 Imperial College London, Department of Life Sciences, Silwood Park Campus, Buckhurst Road, Ascot, SL5 7PY, UK

7 Smithsonian Tropical Research Institute, 0843-03092, Balboa, Ancon, Republic of Panama

8 School of Geosciences, University of Edinburgh, Crew Building, Kings Buildings, Edinburgh EH9 3FF, United Kingdom

9 Forest Research Centre, Sabah Forestry Department, 90715 Sandakan, Sabah, Malaysia.

10 Newcastle University, School of Natural and Environmental Sciences

11Research School of Biology, Australian National University, ACT 2602 Australia

Keywords – Tropical forests, spectroscopy, girdling, tree mortality, traits, drought, el Niño

Abstract – Do tropical trees close to death have a distinct leaf spectral signature? Tree mortality rates have been increasing in tropical forests globally which is reducing the global carbon sink. Upcoming hyperspectral satellites could be used to predict regions close to experiencing extensive tree mortality during periods of stress like drought. Here we show how imminent tropical tree mortality in Borneo impacts leaf physiological traits and reflectance. We measured leaf reflectance (400-2500 nm), light saturated photosynthesis (A_{sat}), leaf dark respiration (R_{dark}), and leaf mass area (LMA) across five campaigns in a six-month period during which there were two causes of mortality: a major drought and a co-incident tree stem girdling campaign. We find that prior to mortality, there were significant ($P<0.05$) leaf spectral changes in the red (650-700 nm), the NIR (1000 -1400 nm) and SWIR bands (2000-2400 nm) and significant reductions in the potential carbon balance of the leaves (increased R_{dark} and reduced A_{sat}). We show that the partial least squares regression (PLSR) technique can predict mortality in tropical trees across different species and functional groups with medium precision but low accuracy (r^2 of 0.65 and RMSE/mean of 0.58). However, most tree death in our study was due to girdling, which is not a natural form of death. More research is needed to determine if this spectroscopy technique can be applied to tropical forests in general.

Introduction

Can future tropical forest tree mortality be predicted with aircraft or satellite remote sensing? This question is of interest because tropical tree mortality is increasing, reducing the global carbon sink (Hubau et al., 2020)(Brienen et al., 2015). Increased tree mortality may be driven by recent increases in extreme weather events caused by climate change, including increased drought frequency/severity (Rifai et al., 2019)(Rifai et al., 2018)(Rowland et al., 2015)(Doughty et al., 2015) or elevated air temperatures (Clark, 2004; Doughty & Goulden, 2009a). Other causes of mortality include altered disturbance regimes due to land management practices or biological invasions (e.g. grass/fire cycles) and the negative environmental impacts arising from forest degradation (e.g. physical damage to trees from logging or small-scale slash-and-burn agriculture; environmental stress from enhanced edges effects) (Malhi et al., 2014). Experimental drought manipulations in the Amazon (Meir et al., 2015)(da Costa et al., 2010; Nepstad et al., 2007) show that larger trees, especially for specific high-abundance taxa (Bittencourt et al., 2020), are more susceptible to mortality. Could changes to leaf properties in these large trees indicate risk of imminent future mortality? Death of these large individuals has the greatest impact on tropical forest vegetation and carbon dynamics (Phillips et al., 2009). "Environmental surveillance" techniques that enable us to identify individuals at risk of death or to predict future patterns of senescence would enable us not only to more accurately model forest vegetation and carbon dynamics, but could possibly enable us to manage the spread of forest pathogens and understand environmental stress gradients related to disturbance. Given that these large trees are also the most visible to aircraft and satellites, remote sensing techniques that enable us to identify dying trees hold tremendous potential for detecting and understanding the causes of tree mortality at large spatial scales.

Leaf traits, like leaf chemistry, photosynthetic capacity or leaf mass per area (LMA), are important indicators of a tree's life history strategy and overall vitality (Poorter et al., 2008; Wright et al., 2004; Wright et al., 2010). Therefore, remote sensing of these traits is one approach that could enable us to detect individuals or taxa at elevated risk of death during stress. For instance, light-demanding species with rapid growth and high mortality rates are predicted to have low seed mass, leaf mass per area, LMA, wood density, and tree height (Wright et al., 2010). Variation in LMA is in part an expression of a trade-off between the energetic cost of leaf construction and the light captured per area that may be reflective of the strategy of the broader tree itself (Díaz et al., 2016; H. Poorter et al., 2009). Drought tolerance is also reflected in structural traits such as LMA, leaf thickness, leaf toughness and wood density, although further studies are required to better establish the limitations of these metrics and identify other potential indices (Bartlett et al., 2012)(Zanne et al., 2010) (Fyllas et al., 2012; Niinemets, 2001).

Is tree death caused by carbon starvation, hydraulic failure, or a combination of the two and what traits are associated with this? To predict tree death with remote sensing we must understand the characteristics that drive tree death. A recent meta-analysis suggests that metrics of hydraulic failure more consistently predicted mortality than carbon starvation as determined by tissue concentrations of NSC (Adams et al., 2017). Another study found hydraulic traits were better at predicting the response of ecosystem fluxes (CO_2 and water vapor) to drought than traits

like LMA or wood density (Anderegg et al., 2018). Tree mortality during droughts is highest for species that have a small hydraulic safety margin (the difference between typical minimum xylem water potential experienced and xylem vulnerability to embolism) (Anderegg et al., 2016). Turgor loss point - the leaf water potential that induces wilting - may be a key trait predicting drought tolerance and species distributions relative to water supply (Bartlett et al., 2012). In tropical forests, there are species-specific changes to turgor loss point at the leaf level (Maréchaux et al., 2015) and xylem pressure at 50% conductivity (xylem-P_{50}), leaf turgor loss point (*TLP*) and cellular osmotic potential (π_o) all occurred at significantly higher water potentials for the drought-intolerant PFT compared to the drought-tolerant PFT(Powell et al., 2017).

Leaf traits can be sensed remotely by aircraft or from space. Foliar traits such as nitrogen (N), chlorophyll content, carotenoids, lignin, cellulose, LMA, soluble carbon, and water can be remotely estimated with leaf spectral reflectance signatures in many different plants and ecosystems (Ustin et al., 2009), including tropical forests (Asner & Martin, 2008). This is because certain traits are associated with reflectance characteristics within specific spectral regions. For instance, the visible part of the spectrum (400–700 nm) is associated with leaf N concentration, and the shortwave infrared (SWIR; 700–1,300 nm) is associated with structures such as palisade cell density. LMA and leaf chemistry have been accurately measured and modelled at both the leaf (one nm bandwidth) (Asner & Martin, 2008; Curran, 1989; Jacquemoud et al., 2009), canopy and landscape scales (at 10 nm bandwidth) (Asner et al., 2016). Other elements not directly expressed in the spectrum, such as phosphorus (P), have been accurately predicted with spectroscopy, possibly through a stoichiometric relationships with other chemical species (Ustin et al., 2006, 2009) or correlations with leaf morphological traits via the leaf economics spectrum (Wright et al 2004). Other tropical tree traits not directly associated with leaf spectra, such as leaf age (Chavana-Bryant et al., 2017), photosynthetic capacity (Doughty et al., 2011), and branch wood density, have been predicted with spectroscopy in tropical forests (Doughty et al., 2017). Predicted traits not directly associated with spectral regions are likely correlations between leaf traits and a tree's life history strategy (Doughty et al., 2017).

There is evidence that drought changes tropical forest reflectance at the continental scale, due to changes in leaf traits or increased tree mortality. For instance, EVI, a greenness index, as measured with Moderate Resolution Imaging Spectroradiometer (MODIS) increased in the Amazon during the 2005 drought (Saleska et al., 2007). However, others have challenged the original interpretation of the EVI data (Morton et al., 2014; Samanta et al., 2010), highlighting the challenge of remote sensing at a continental scale. More recently, during a major El Niño drought in Borneo, NDVI initially increased as the drought was strengthening, but decreased at its peak (Nunes et al., 2019). Interpretation of changing NDVI and/or EVI, at a larger spatial scales is generally complicated in many ecosystems as changes at the leaf level may be compensated for or masked by branch level process, for example leaf senescence and drop may reduce the canopy scale NIR signal. However, remotely sensed LAI signal saturates in tropical forests and LAI variation can be relatively small even following strong climate extremes such as drought. For instance, Meir et al. 2018 found a 12-20% change in LAI during an extreme

drought manipulation experiment with a ~5.5 m^2 m^{-2} LAI which is within the saturation range. Therefore, changes in tropical forest canopy spectral characteristics at larger spatial scales may be more linked to changes changes in leaf level spectra, than in other ecosystems (Doughty & Goulden, 2009b; Wu et al., 2018).

The 2016 El Niño caused a significant drought in Borneo, both in terms of increased temperature and reduced precipitation (Figure 1)(Rifai et al., 2019)(Rifai et al., 2018). This El Niño had unusually high temperatures, which have been attributed to a climate change-amplified El Niño event (Thirumalai et al., 2017). Recent work in Borneo, near our study site, found the El Niño event was associated with a decrease in chlorophyll and carotenoid concentrations by 35% (as NDVI decreased), and this was reflected in the shortwave infrared region of leaf spectral signatures (Nunes et al., 2019). These authors hypothesized that trees produced new leaves with higher pigment concentrations at the start of the El Niño event, and then dropped their leaves at its peak.

In this study, we focus on tree mortality at a 1 ha long-term study site close to the Nunes et al 2019 study in Sabah, northern Borneo. We attempt to understand the relationship between leaf traits, spectroscopy and mortality in two different ways: natural death during El Niño and forced mortality induced by girdling. Before, during and after the 2016 El Niño drought (over 5 field campaigns), we measured canopy-top leaf spectroscopy (400-2500 nm), leaf level gas-exchange photosynthesis, dark respiration and LMA in a representative cross section of the 393 monitored trees. We further tried to explore mechanisms of mortality with a girdling campaign (the removal of the phloem in a 10 cm ring around the tree stem) in one half (0.5 ha, 210 stems) of the plot. Here, we test the following hypotheses:

H1 – Leaf traits that are correlated with leaf spectroscopy signals, such as light saturated photosynthesis, dark respiration, and LMA, change months prior to tree mortality.

H2 - Tropical tree mortality can be predicted with hyperspectral information (400-2500 nm 1 nm bandwidth leaf reflectance).

Methods

Study sites

Our study plots are in Kalabakan Forest Reserve in Sabah, Malaysian Borneo (Tower SAF-05 4.716°, 117.609°) within the Stability of Altered Forest Ecosystems (SAFE) Project (Ewers et al., 2011; Riutta et al., 2018). A schematic of the study site is shown in figure 1C. Mean annual temperature is approximately 26.7°C and mean annual precipitation is 2,600–2,700 mm with no distinct dry season but ~12% of months with precipitation below 100 mm month^{-1} (Walsh & Newbery, 1999). The plot has been selectively logged four times since the 1970s, which represents a high logging intensity for this region. The soils are orthic Acrisols or Ultisols on undulating clay soil. Tree basal area is 13.9 m^2/ha. Total NPP and autotrophic respiration has been measured at the plot since 2011 and there is an eddy covariance tower nearby (Riutta et al., 2018). The plot is split in half by a small stream. All the trees on one side of the stream were girdled in late Jan, 2016 by removing the phloem tissue in a 10 cm band, as described below (note: the plot was in the process of conversion to oil palm agriculture production). This part of the study site is hereafter referred to as the "girdled plot." The trees on the other side of the stream were not girdled and represent the treatment control. This part of the study site is hereafter referred to as the "drought plot". Although all trees experienced drought, the "drought" plot only experienced drought and not the effects of girdling. We collected data during five field campaigns that took place from January to June 2016 (i.e. Campaign 1=21 Jan-16, Campaign 2=10 Feb-16, Campaign 3=01 Mar-16, Campaign 4=29 Mar-16, Campaign 5 08 Jun-16). The first field campaign (C1) was conducted before girdling occurred to determine pre-girdling conditions and process rates.

Girdling experiment – In late Jan 2016, after the first field campaign, we further explored the causes of tree mortality by conducting a girdling experiment. Girdling involved removing a 10 cm strip of the periderm and phloem in a ring around the tree stem at ~1.2 m height (with exceptions for trees with buttresses, which were girdled above the buttress) above the soil (Figure 1a) in a plot that was scheduled for conversion to a Palm Oil plantation. This technique prevents carbohydrate transport to the roots, but maintains hydraulic connectivity because xylem tissue are not severed. Tree death was determined visually, based on the absence of visible canopy, with regular (average 18 day period) visits to the plots for both the drought and the girdled plots. We give the species measured in both plots in Table 1.

Leaf sampling strategy –In each plot, 20-25 trees were chosen during each campaign, and tree climbers with extendable tree pruners removed one branch per tree that was growing in full sunlight. These branches were quickly recut underwater and returned to a central lab building for further measurements. On each of these branches, five fully expanded non-senescent leaves in randomly selected locations were chosen for measurements of: leaf-gas exchange (respiration and photosynthesis), and dark respiration, leaf spectral properties (measured within 1 hour of being cut) and LMA. Leaf area was determined immediately after collection using a digital 476 scanner (Canon LiDE 110) and then oven dried at 72 °C until constant mass was reached.

Leaf-level gas exchange – We used a portable gas exchange system (LI 6400, Li-Cor Biosciences, Lincoln, NE, USA) to measure leaf-level gas exchange. After returning to the central lab building, leaf dark respiration (R_{dark}) was measured by covering branches with an

opaque bag for at least 20 minutes prior to measurement at a cuvette temperature of 30° C. After this, branches were exposed to sunlight and light-saturated leaf photosynthesis was measured (A_{sat}; 1200 µmol m^{-2} s^{-1} PPFD, 400 ppm CO_2, at 30° C). With A_{sat}; 1200 µmol m^{-2} s^{-1} chosen because photosynthetic capacity in most tropical leaves saturates above light levels of 1200 µmol m^{-2} s^{-1} PPFD (Both et al., 2019; Gvozdevaite et al., 2018)(Doughty & Goulden, 2009b). We waited for gas exchange values to stabilize before starting a measurement, recorded data every 2 seconds and averaged the results after eliminating the first 20 measurements. We excluded photosynthesis measurements less than 0 µmol m^{-2} s^{-1} (as this was indicative of a failure to maintain hydraulic connectivity in the sampled branch resulting in stomatal closure) and dark respiration measurements more negative than -1.5 µmol m^{-2} s^{-1} (as this was considered indicative of a failure to truly represent $R_{d,}$ or in some cases operator error). Most physiological measurements were collected between 07:00 and 14:00 local time and branches were cut from tree between 06:00 and 13:00 local time. An online supplement includes our averaged ± sd data for each leaf measured for transpiration rate (mmol H_2O m^{-2} s^{-1}), vapor pressure deficit based on leaf temp (kPa), intercellular CO_2 concentration (µmol CO_2 mol-1), conductance to H_2O (mol H_2O m^{-2} s^{-1}), and photosynthetic rate (µmol CO_2 m^{-2} s^{-1}).

Leaf spectroscopy – We randomly selected five leaves within an hour of each branch being cut and measured hemispherical reflectance near the mid-point between the main vein and the leaf edge. We used an ASD Fieldspec 4 with a fibre optic cable, contact probe and a leaf clip (Analytical Spectral Devices High Intensity Contact Probe and Leaf Clip, Boulder, Colorado, USA). The spectrometer records 2175 bands spanning the 325–2500 nm wavelength region. Measurements were collected with 136-ms integration time per spectrum. To ensure measurement quality, the spectrometer was calibrated for dark current, stray light and white referenced to a calibration panel (Spectralon, Labsphere, Durham, New Hampshire, USA) after each branch. The spectrometer was optimized after every branch. For each measurement, 25 spectra were averaged together to increase the signal-to-noise ratio of the data.

Data analysis - We used the Partial Least Squares Regression (PLSR) modelling approach to predict leaf traits with spectral information, (Geladi & Kowalski, 1986). PLSR incorporates all the spectral information within each leaf reflectance measurement, eventually reducing all spectral data (400-2500 nm) down to a relatively few, uncorrelated latent factors. This approach has been used successfully to predict plant traits across a wide range of ecosystems, including tropical forests (Asner & Martin, 2008)(Serbin et al., 2014). We used the PLSregress command in Matlab (Matlab, MathWorks Inc., Natick, MA, USA) to establish predictive models for LMA, Asat, wood density and tree mortality. We minimized the mean square error with K-fold cross validation to avoid over-fitting the number of latent factors. To create a completely independent testing dataset, we used the above method on 70% of our data to calibrate our model and then the remaining 30% to test the accuracy of our model. We evaluated the accuracy of our modelled estimates using two main metrics: r^2 and root mean square error (RMSE)/mean. We grade our results as high precision and accuracy ($r^2 > 0.70$; %RMSE < 15%), medium precision and accuracy ($r^2 > 0.50$; %RMSE < 30%), low precision and accuracy ($r^2 > 0.50$; %RMSE > 30%).

Statistical tests – For our leaf spectral measurements, for each 1 nm bandwidth, we determined statistical significance ($P<0.05$) with a paired t-test. To understand significant differences between differences of LMA, R_{dark}, and A_{sat}, we used a t-test. To understand the impact of the girdling over time, we used a repeated measures ANOVA.

Results

The field campaigns overlapped with the 2016, El Niño in Borneo (Figure 1b). Campaign 1 (C1- Jan-21) was before the period with peak drought and temperature, C3 (March - 16) was the peak of the drought and high temperatures, and by C5 (June-16) the rains had returned. After C1, all the trees in the girdled plot had their phloem tissue removed in a 10 cm band. Given the downward flux of sugars from the canopy, we might expect an initial build-up of sugars above the girdle followed by eventual tree death as carbon starvation below the girdle impacts tree function, particularly in the roots. Companion papers explore the causes of tree death and the impacts on plant hydraulics and soil respiration.

There was little change in leaf reflectance (400-2500 nm) between C1 and C2 (Figure 2) in both the drought and girdle plots. We expected few spectral changes during this short interval between C1 and C2 (Jan-21 to Feb-10) for the natural drought plots, but we were surprised there were also few changes for the girdled plots since these trees experienced a significant trauma. In the later campaigns (C3 to C5 01-Mar to 08-Jun), there were large (~0.03 albedo units) decreases in NIR reflectance (750-1500 nm) in both the girdled and natural drought plots (Figure 2 a and b). Reflectance in the visible wavelengths were greater during the peak natural drought (C3) than after the rains returned (C4 and C5). The girdled plots showed a consistent decrease in the visible bands. The SWIR bands also differed between girdled and drought (non-girdled), with large decreases in the drought plots and little change in the girdle plot except for the final campaign where there was an increase. However, changes in spectral properties in the girdled plot might also have resulted from species changes because certain tree species died sooner than others, thus changing the species composition as the experiment continued.

Our average A_{sat} values across the campaigns for the girdled plot (3.7 μmol CO_2 m^{-2} s^{-1}) and the drought plot (4.7 μmol CO_2 m^{-2} s^{-1}) were slightly lower, but within 95% confidence intervals of values from a nearby campaign in Borneo of community weighted mean and 95% confidence interval of 4.08 μmol CO_2 m^{-2} s^{-1} (2.7–5.5) for the old growth plots and 7.0 μmol CO_2 m^{-2} s^{-1} (5.7–8.4) for the selectively logged plots (Both et al., 2019). Our average R_{dark} values across the campaigns for the girdled plot (-0.82 μmol CO_2 m^{-2} s^{-1}) and the drought plot (-0.83 μmol CO_2 m^{-2} s^{-1}) were likewise slightly lower than the values from Both et al 2019 of –1.0 μmol CO_2 m^{-2} s^{-1} (–0.9 to –1.2) for the old growth plots and –1.3 μmol CO_2 m^{-2} s^{-1} (–1.1 to –1.4) for the selectively logged plots. Light saturated leaf photosynthesis and R_{dark} showed strong seasonality in both plots over the measurement period (Figure 3). For instance, A_{sat} increased in both the drought and girdled plots in campaign 5 following the return of the rains. Surprisingly, the surviving girdled trees had the highest photosynthetic rates of the campaign in C5 despite the damaged phloem. Dark respiration was at its lowest in C3 and 4 during the peak of the drought. In both groups, changes in R_{dark} matched those in A_{sat} meaning that as A_{sat} increased so did dark respiration. The ratio R_{dark}/ A_{sat} showed a similar seasonal cycle, with the exception of C4, which was less efficient in the drought plot. A repeated measures ANOVA showed no significant differences between A_{sat}, R_d, and LMA over time between the girdled and drought plots across the five campaigns suggesting the girdling had little overall impact of on leaf physiology.

Details of the trees that died (i.e. size, species, functional traits) is the topic of a companion paper (Nottingham et al in prep), but functional traits, such as wood density, may explain some of the timing of tree mortality in our study (see companion paper). To understand

how the drought and girdling impacted leaf spectral properties in different ways according to functional traits, we binned our results into groups of trees with either high (>0.5 g cm^3) or low wood density (<0.5 g cm^3) (Figure 4). Tree species with lower density wood showed a much stronger reaction to the drought in the NIR and SWIR bands than tree species with higher density wood, with fewer significant changes ($P<0.05$) in the visible bands. In contrast, the high wood density tree species show a stronger reaction to the girdling than the low wood density species, again with most of the change in the NIR and SWIR bands.

We then compared near death leaf reflectance (within 50 days of dying) to leaf reflectance from the same trees not near to death (Figure 5). We found that as death approaches in the girdled trees, there are large, significant reductions in reflectance in the visible, the red edge and most of the NIR ($P<0.05$). By C5, 38 trees or 18% percent of all girdled trees had died. There were large (0.03-0.05 reflectance units) and significant decreases ($P<0.05$) in leaf reflectance in the visible bands and the red edge as tree death approached. There were also large (0.02) and significant increases ($P<0.05$) in leaf reflectance in NIR and SWIR bands too. Next, we investigated how drought conditions, precipitated by the ENSO event, affected leaf spectral properties in trees which died naturally in the non-girdled control plot. Only one tree died from drought in the control that was intensively sampled for functional traits. We observed similar significant changes in this tree as observed in the trees that died following the girdling treatment: reductions in reflectance occurred in the red, the NIR and SWIR bands. However, there was a significant peak in the red edge in the opposite direction compared to the girdling study. The wavelengths that show similarities for both types of death are: red (650-700nm), the NIR (1000 - 1400nm) and SWIR bands (2000-2400nm).

For both the girdled and non-girdled trees, there were highly significant changes ($P<0.0001$) to the potential carbon balance (R_{dark} /A_{sat} – Figure 6e and f) of the leaves just prior to death (i.e. within 50 days). In both the drought and the girdled plots, there were significant increases in R_{dark} and significant decreases in A_{sat} (Figure 6). This combination of increased respiration and decreased photosynthesis should reduce the carbon available to the tree (again dependent on stomatal conductance changes). There was no significant change in LMA with the girdled trees. In contrast, in the tree that died from drought in the non-girdled plot, the leaves had significantly higher LMA near to death. We do not know if this was a result of a changing cohort of leaves present on the sampled branch (i.e. leaves with lower LMA senesced sooner) or if all leaves changed their LMA via altered density prior to death (but this is less likely as structural carbon is fixed).

Finally, we used PLSR to predict changes in physiology and time to death with spectroscopy (Figure 7). We used the primary weighting (right side of figure 7) to understand which spectral regions are most important (deviations from 0). Spectroscopy predicted LMA with an r^2 of 0.70 and RMSE/mean of 0.14 (similar to many other studies with high precision and high accuracy (Asner and Martin 2008, Doughty et al 2011). The primary weighting is in the NIR and SWIR bands which is typical of traits relating to structure. Spectroscopy predicted maximum photosynthetic rate (A_{sat}) with an r^2 of 0.65 and RMSE/mean of 0.69 (medium precision but low accuracy) and wood density with an r^2 of 0.45 and RMSE/mean of 0.24 (low

335 precision but medium accuracy). The primary weighting of A_{sat} was in the visible bands (likely
336 related to chlorophyll content) and for wood density in NIR and SWIR >1000 nm (likely related
337 to variations in LMA and leaf structure). Finally, we predicted to time to death with spectroscopy
338 and the PLSR technique with an r^2 of 0.65 and RMSE/mean of 0.58 (medium precision and low
339 accuracy). The primary weighting shows similarity with Figure 5 with important spectral
340 regions in the visible (related to photosynthetic characteristics), the NIR (related to structure) and
341 SWIR bands (related to water bands).

342

343

Discussion

Leaf spectroscopy - Identification of tropical trees susceptible to mortality through hyperspectral imagery could provide a powerful tool in examining recently reported increases in tree mortality rates across the tropics (Hubau et al., 2020)(Brienen et al., 2015). By contributing to "environmental surveillance," the use of hyperspectral data would have a wide range of applications from the prediction of tree death from heat stress, pests, pathogens or illegal logging. Moreover, this technique could enable us to identify potential tipping points in tropical forests, with wider ramifications for the development of adaptive forest management strategies in the future. Based on these preliminary results, future mortality is potentially predictable using hyperspectral imagery for up to 50 days in advance of tree death (Figure 7). We also observed a tree that died naturally from drought, and saw that there were regions of spectral overlap with the signal from trees killed by girdling in terms of the wavelengths that changed prior to tree death; e.g. red (650-700nm), the NIR (1000 -1400nm) and SWIR bands (2000-2400nm) (Figure 5). This gives us some confidence that the spectral changes may be general to mortality and not specific to girdling-induced mortality. We demonstrate only changes in leaf reflectance and not overall canopy reflectance. It is important to differentiate between leaf versus canopy reflectance (as seen from aircraft or space) because the latter also incorporates forest structural changes (like variations in LAI and branch architecture), which we have not measured. Leaf spectral properties strongly influence canopy spectral properties especially in certain wavelengths (Asner and Martin 2008), but changes in other properties, like LAI, could confound the signal. Large shifts in these spectral regions may be indicative of tree mortality and should be tested with hyperspectral aircraft data in the region for confirmation (Swinfield et al., 2019).

Surprisingly, leaf spectral properties did not vary greatly during the period immediately following tree girdling (~1 week). Previous studies have quantified changes in non-photosynthetic vegetation to estimate regional selective logging (Asner et al., 2005). Here we show that significant trauma to the trunk did not immediately result in changes to leaf spectral properties but leaf spectral properties did change within 50 days of tree death. We hypothesize that > 10 days is the time needed to change the biochemistry, physiology and metabolism of leaves to respond to environmental stress. This indicates that >10 days but <50 are necessary for leaf spectral changes to occur (Figure 5), which could constrain timing for a potential new technique to identify damage to trees from selective logging.

It should be noted that our plots had been extensively logged, four times since the 1970's with 46 to 54 Mg C ha^{-1} cumulative extracted biomass in the area (Riutta et al., 2018). This has been shown with hyperspectral imagery to lower canopy foliar nutrient concentrations and decrease nutrient availability (Swinfield et al., 2019). Our results are therefore biased towards logged/low foliar nutrient forests, although our dataset does include late-successional species as well. However, most forests (72%) in the region have been selectively logged, and our results should be valid for these forests (Bryan et al., 2013).

Leaf physiology - Dark leaf respiration, R_{dark}, was at its lowest during the peak of the drought, in campaigns C3 and C4. This stands in contrast to other leaf respiration studies during an artificial drought that saw a strong increase in leaf respiration rates (Rowland et al., 2015), although recent results suggest that this response may be taxon-specific result that is not observed across all

species (Rowland et al in review). Leaf R_{dark} also did not increase in the girdled leaves despite potential increases in leaf NSCs (as they could not be transported towards the roots following the girdling). Other studies have shown a decrease in overall respiration during drought periods as compared to before a drought (Doughty et al., 2015), and this is a similar pattern shown at our plots (Riutta et al 2020).

We also observed both increased R_{dark} and decreased A_{sat} 50 days prior to tree death, which in combination are very likely to reduce the carbon available in leaf tissue (although net carbon balance is also dependent on changes in stomatal conductance). Which in turn could increase the likelihood of carbon starvation (McDowell et al., 2018) and reduce the availability of carbon (or more accurately NSC) for embolism repair the of reversal of in the water conducting xylem tissue (Sala et al., 2012). It is also interesting to note that the highest average photosynthetic capacity (A_{sat}) for the girdled experiment were observed when the rains returned. We speculate that might be due to a growth or sink driven response where, after the return of available water increased growth (e.g. fine root growth and leaf flushing) to replace senesced tissue results in a higher carbon sink leading to a a higher demand for NSC with a consequent increase in A_{sat}. Overall, this is more evidence that photosynthesis is robust despite perturbations, and that growth may be maintained preceding a mortality event as the plant attempts to recover damaged xylem capacity (L. Rowland et al., 2015; Lucy Rowland et al., 2015).

Conclusion

Our key finding is that remote sensing using spectral imagery shows potential to identify trees at imminent risk of death (approximately 50 days prior). This technique has widespread relevance and applicability for ecological/management surveillance, prediction of future vegetation and forest carbon dynamics. We suggest aircraft campaigns search for a large shift in visible, red edge, and NIR reflectance and compare this to observed tree mortality. For instance, we hypothesize that comparing hyperspectral aircraft flights before and after the 2016 drought might show large shifts in reflectance properties prior to tree mortality (Davies et al., 2019)(Swinfield et al., 2019). This could also be of use for hyperspectral satellites (Krutz et al., 2019). The large significant changes in leaf reflectance observed here that were shared by both girdling- and drought-killed trees at the same timescale prior to mortality indicate that there could be a spectral indication of tropical tree mortality that has regional or wider application.

Acknowledgements – We would like to acknowledge Dr. Rob Ewers for his role in setting up the SAFE experiment, Elelia Nahun, Dg Ku Shamirah binti Pg Bakar for their contributions to the field campaign, Unding Jami, Ryan Gray, Rostin Jantan, Suhaini Patik and Rohid Kailoh and the BALI and Lombok project research assistants.

Tables

Table 1 – Tree species measured intensively in the drought and girdled plot aligned to show which species were measured in both plots.

Girdled Plot	Drought Plot
Adinandra borneensis,	*Adinandra borneensis,*
Brownlowia peltata,	
	Cariumna odontophyllum,
	Diplodiscus paniculatus,
	Dipterocarpus caudiferus,
Dryobalanops lanceolate,	*Dryobalanops lanceolate,*
Duabanga moluccana,	*Duabanga moluccana,*
	Endospermum peltatum,
Hydnocarpus anomalus,	
Leea aculeate,	
Lithocarpus blumeanus,	*Lithocarpus blumeanus,*
Litsea garciae,	
Lophopetalum sp.,	
Macaranga hypoleuca,	
Macaranga pearsonii,	*Macaranga pearsonii,*
	Mallotus leucodermis,
	Nauclea officinalis,
Neolamarckia cadamba,	*Neolamarckia cadamba,*
Nephelium rambutan,	
Parashorea malaanonan,	*Parashorea malaanonan,*
	Pleiocarpidia sandakanica,
	Pterospermum elongatum,
	Shorea gibbosa,
Shorea johorensis,	*Shorea johorensis,*
Shorea parvifolia.	
	Syzygium sp.,
	Trema orientalis

Figures

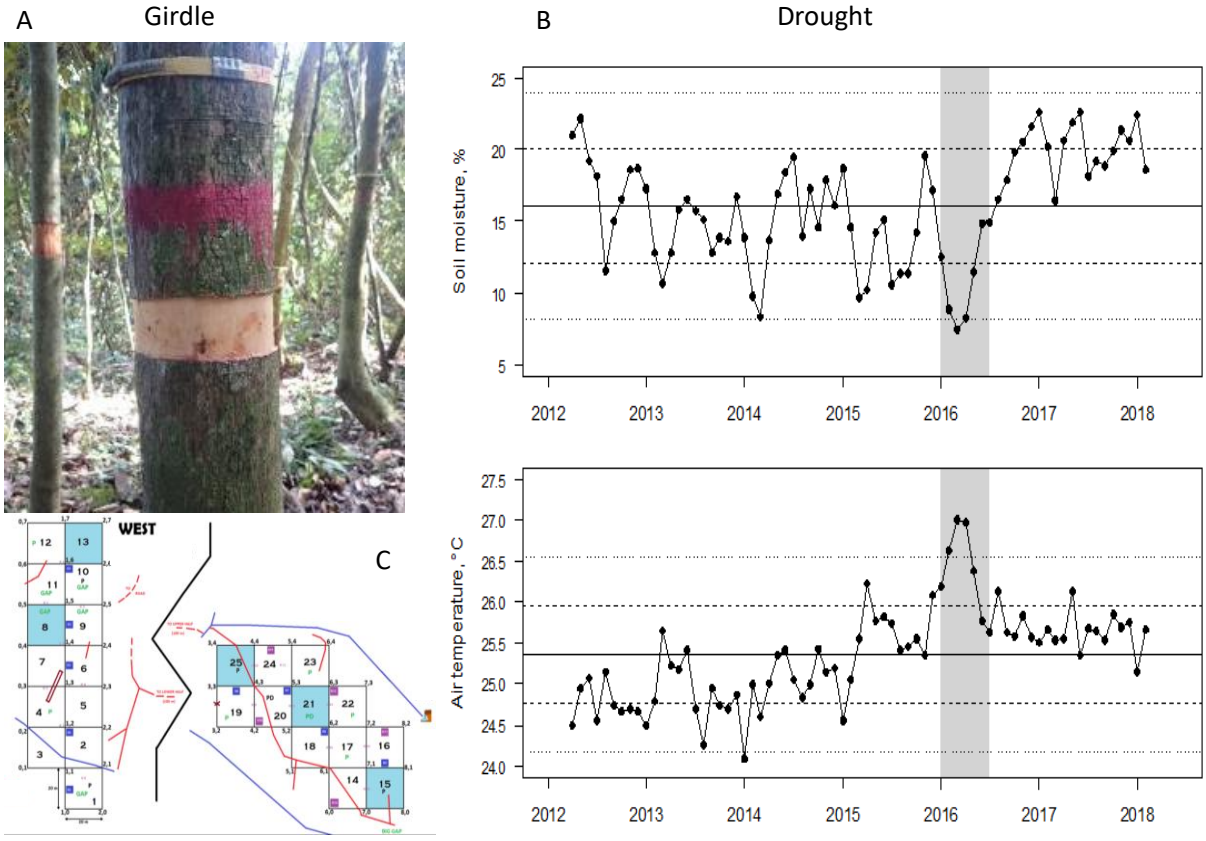

Figure 1. (A) An example tree that was girdled by stripping 10 cm of phloem in a ring around the tree. (B) Monthly volumetric soil moisture content at 20 cm depth (top) and air temperature (bottom) records at the study site. The horizontal continuous line denotes the long-term mean and the dashed lines denote 1 and 2 standard deviations. The grey region is the period of our measurements. (C) A schematic of the plot layout with the non-girdled trees in the section labelled West (the other section was girdled). The total area of the plot is 1 ha, with the two sections separated by approximately 200 m. The middle black line represents the river. Each individual square represents a 20 m ×20 m subplot. Red lines are trails and blue lines are small temporary streams.

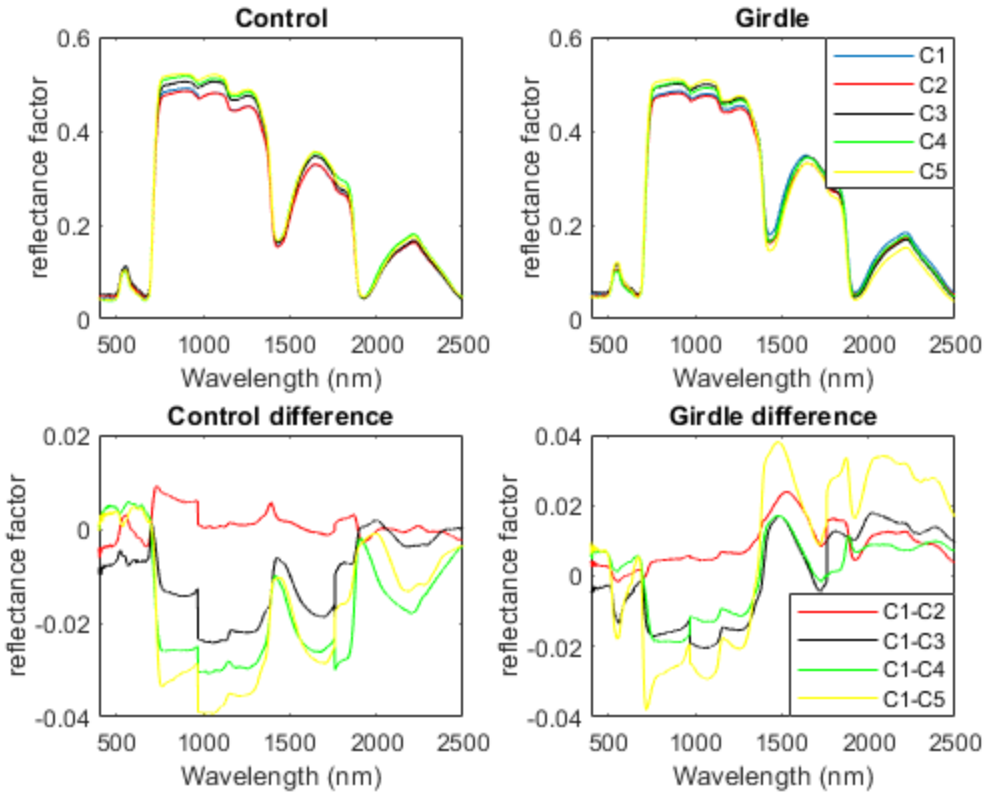

440

441 **Figure 2.** Leaf spectral properties (400-2500nm) for the drought (left) and girdled (right) plots for the 5
442 campaigns (Jan-June 2015). (bottom) The difference (C1-CX, where X=2-5) in leaf spectral properties
443 for the control (left) and the girdled (right) plots. In each campaign, we sampled the same trees unless the
444 trees died. Reflectance factor is reflected incident light between 0-1.

445

446

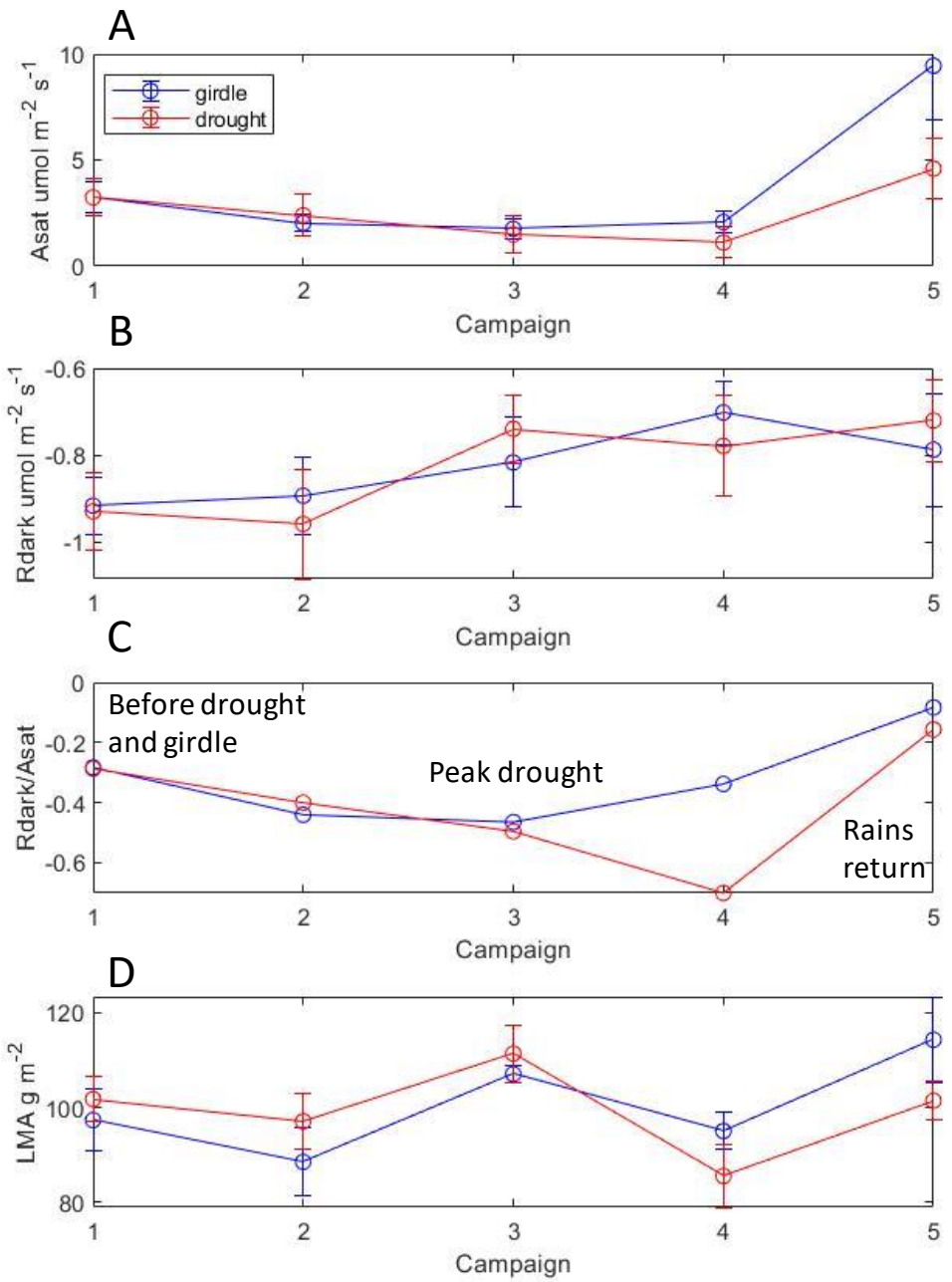

Figure 3. Average ± se (A_{sat}) photosynthetic capacity (A), (R_{dark}) leaf dark respiration (B), A_{sat} / R_{dark} (C) and (LMA) leaf mass area (D) for the 5 campaigns for the control site (red) and the girdled site (blue). A_{sat} and R_d were collected at a standard temperature (30 °C) during all campaigns. We subtracted the initial difference (2 µmol m^{-2} sec^{-1}) in the top panel between the average C1 values to better highlight the impact of the girdling.

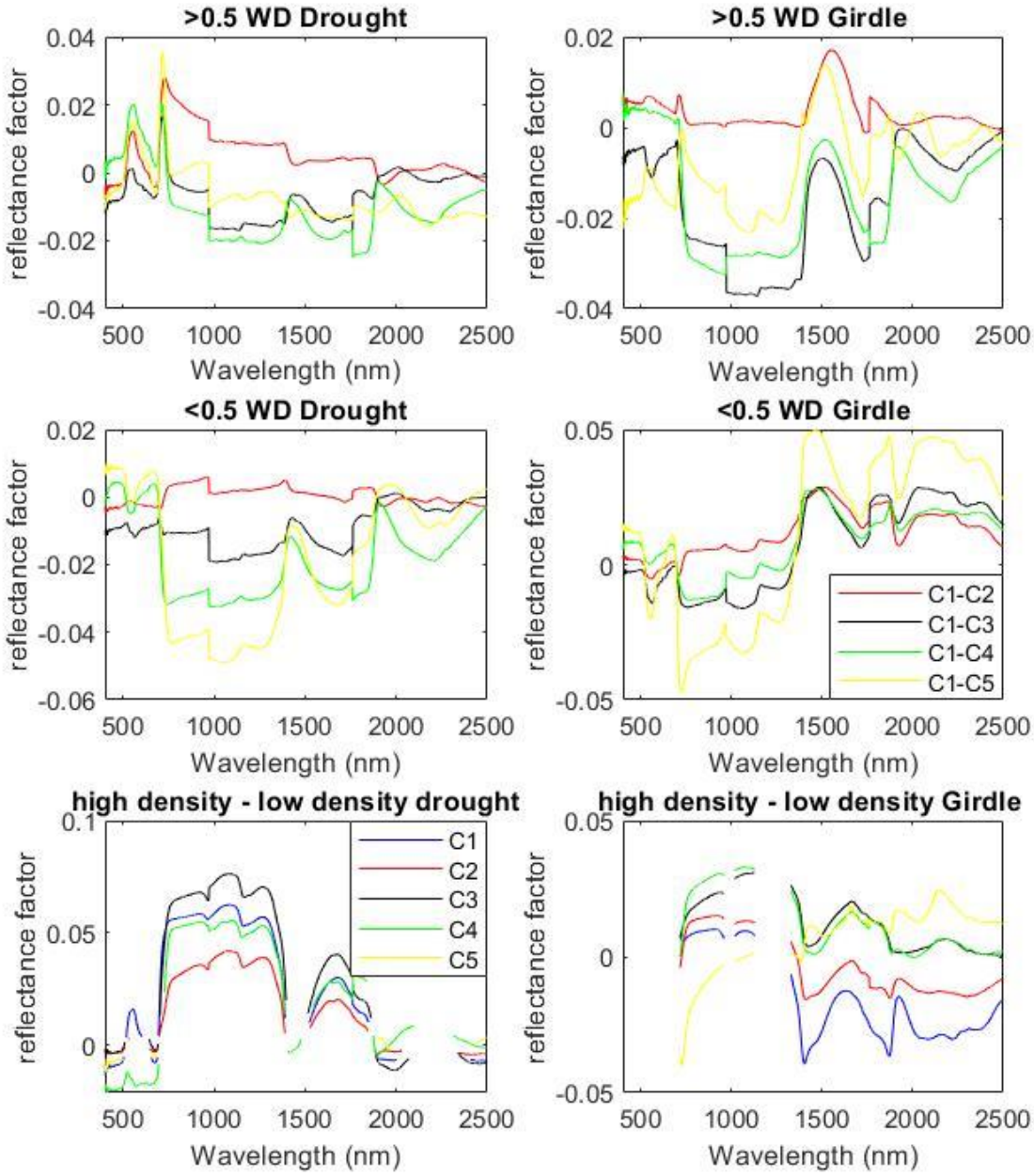

456

457 **Figure 4.** Leaf spectral properties (400-2500nm) comparing low wood density (density<0.5 g cm^{-3}, left)
458 and high wood density species (density >0.5 g cm^{-3}, right) through the 5 Campaigns for the control plot
459 (top) and the girdled plot (middle). For each campaign, we subtract dense wooded species from light
460 wooded species (bottom). Only significant spectral regions are shown in the bottom.

461

462

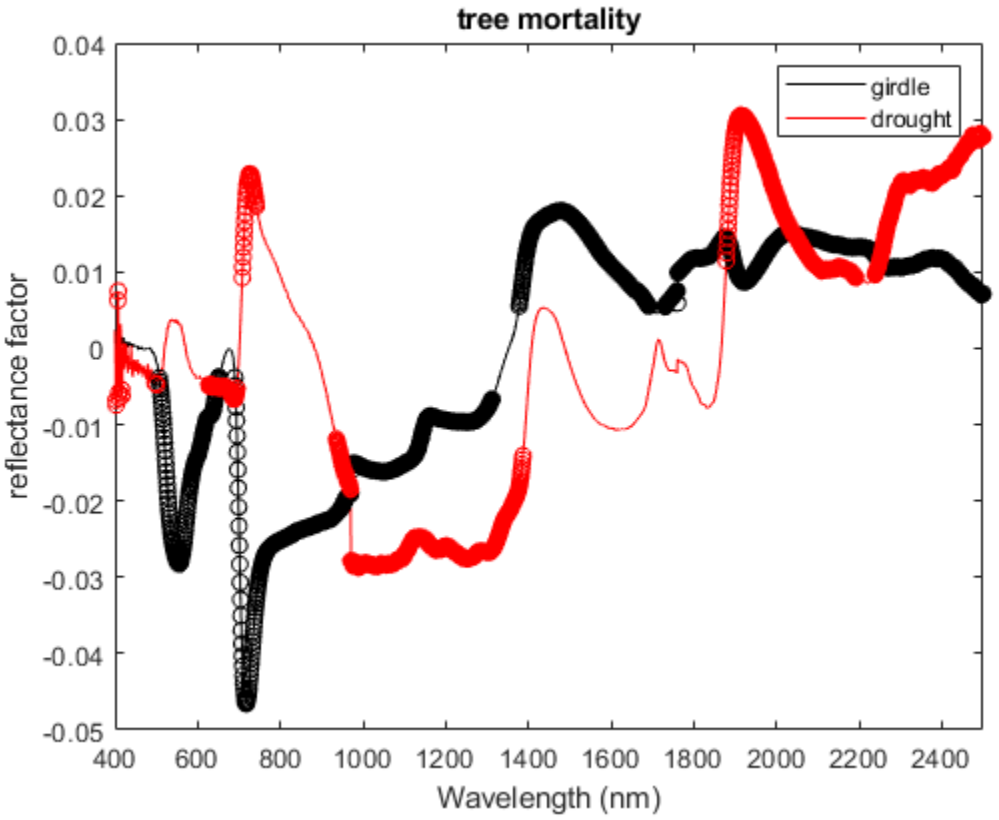

Figure 5 –The change (negative is a reduction in reflectance close to death) in leaf spectral properties from healthy leaves (>50 days from death) minus close to death leaves (<50 days from death) on a tree that died of natural drought (red, N=14 leaves) and trees that died during the girdling experiment (black, N=122 leaves). Dots show regions of significant change (P<0.05) using a paired t-test.

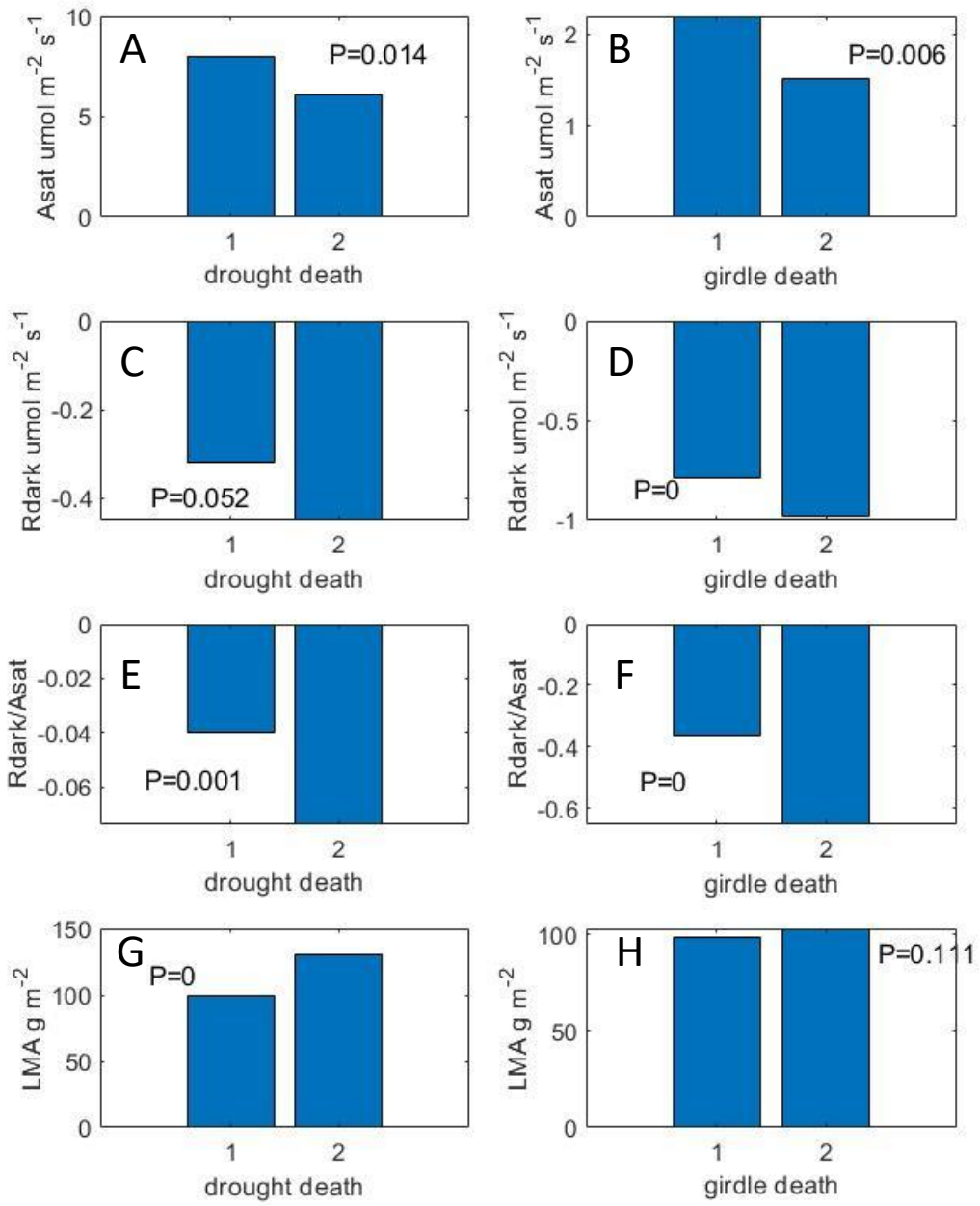

473

474 **Figure 6** – Comparison of A_{sat} (A), R_{dark} (C), R_{dark}/ A_{sat} (E) and LMA (G) between initial values
475 (1) and values within 50 days of death (2) for the girdling experiment (right) and the intensively
476 monitored tree that died during the drought (left). The P value listed is the level of significance
477 to three digits for a student's t-test.

478

479

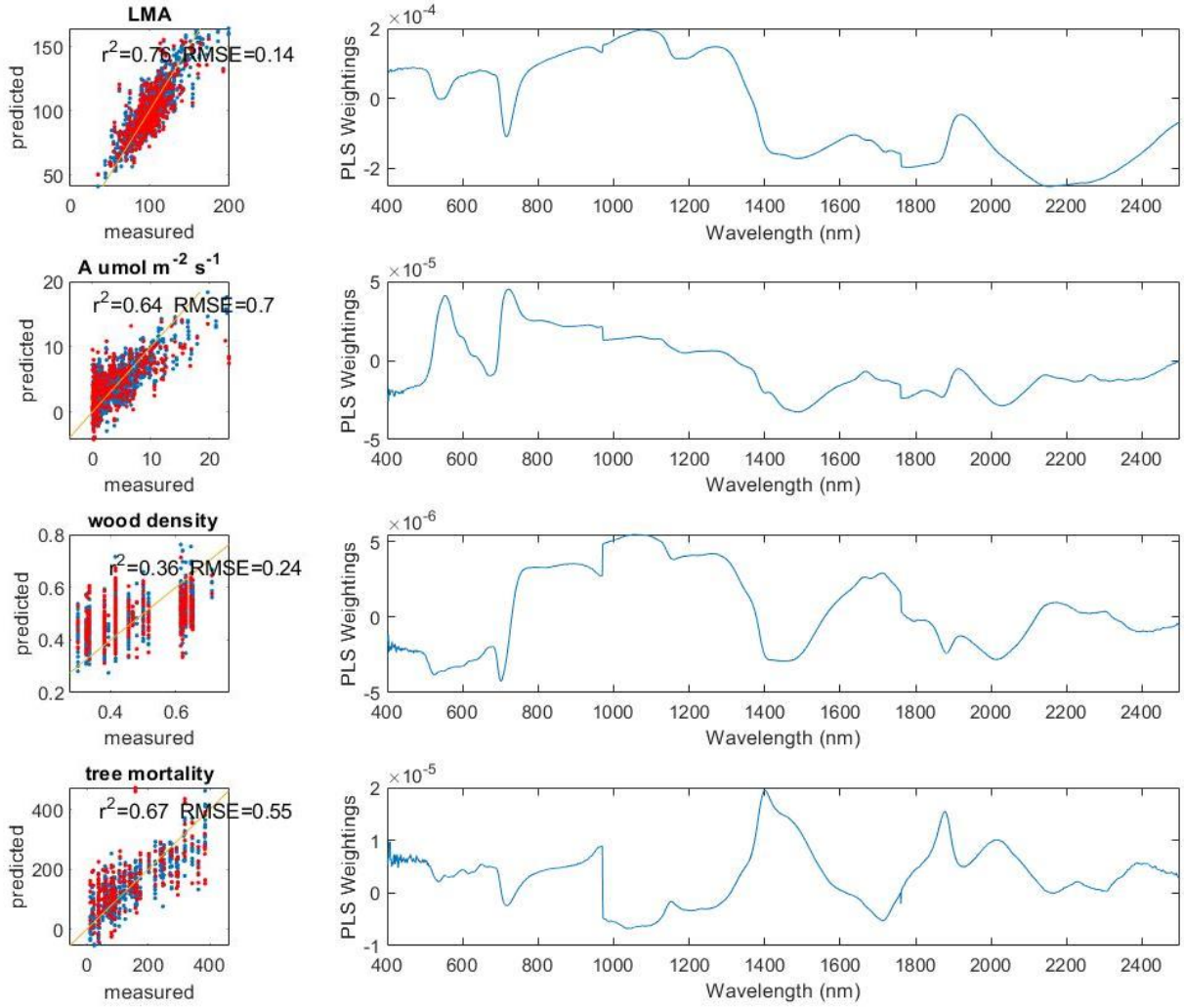

480

481 **Figure 7.** Results from our PLSR analysis where we try and predict various traits including LMA,
482 photosynthesis, wood density, and time to tree death. Red dots are the data to train the model (70%) and
483 the blue dots are the independent dataset (30%). On the right is the primary weighting and on the left is
484 the predictive power (measured vs predicted) with the r^2 and RMSE/mean.

485

References

Adams, H. D., Zeppel, M. J. B., Anderegg, W. R. L., Hartmann, H., Landhäusser, S. M., Tissue, D. T., et al. (2017). A multi-species synthesis of physiological mechanisms in drought-induced tree mortality. *Nature Ecology and Evolution*. https://doi.org/10.1038/s41559-017-0248-x

Anderegg, W. R. L., Klein, T., Bartlett, M., Sack, L., Pellegrini, A. F. A., Choat, B., & Jansen, S. (2016). Meta-analysis reveals that hydraulic traits explain cross-species patterns of drought-induced tree mortality across the globe. *Proceedings of the National Academy of Sciences of the United States of America*. https://doi.org/10.1073/pnas.1525678113

Anderegg, W. R. L., Konings, A. G., Trugman, A. T., Yu, K., Bowling, D. R., Gabbitas, R., et al. (2018). Hydraulic diversity of forests regulates ecosystem resilience during drought. *Nature*. https://doi.org/10.1038/s41586-018-0539-7

Asner, G. P., & Martin, R. E. (2008). Spectral and chemical analysis of tropical forests: Scaling from leaf to canopy levels. *Remote Sensing of Environment*. https://doi.org/10.1016/j.rse.2008.07.003

Asner, G. P., Knapp, D. E., Broadbent, E. N., Oliveira, P. J. C., Keller, M., & Silva, J. N. (2005). Ecology: Selective logging in the Brazilian Amazon. *Science*. https://doi.org/10.1126/science.1118051

Asner, G. P., Knapp, D. E., Anderson, C. B., Martin, R. E., & Vaughn, N. (2016). Large-scale climatic and geophysical controls on the leaf economics spectrum. *Proceedings of the National Academy of Sciences of the United States of America*. https://doi.org/10.1073/pnas.1604863113

Bartlett, M. K., Scoffoni, C., & Sack, L. (2012). The determinants of leaf turgor loss point and prediction of drought tolerance of species and biomes: A global meta-analysis. *Ecology Letters*. https://doi.org/10.1111/j.1461-0248.2012.01751.x

Bittencourt, P. R. L., Oliveira, R. S., da Costa, A. C. L., Giles, A. L., Coughlin, I., Costa, P. B., et al. (2020). Amazonian trees have limited capacity to acclimate plant hydraulic properties in response to long-term drought. *Global Change Biology*. https://doi.org/10.1111/gcb.15040

Both, S., Riutta, T., Paine, C. E. T., Elias, D. M. O., Cruz, R. S., Jain, A., et al. (2019). Logging and soil nutrients independently explain plant trait expression in tropical forests. *New Phytologist*. https://doi.org/10.1111/nph.15444

Brienen, R. J. W., Phillips, O. L., Feldpausch, T. R., Gloor, E., Baker, T. R., Lloyd, J., et al. (2015). Long-term decline of the Amazon carbon sink. *Nature*. https://doi.org/10.1038/nature14283

Bryan, J. E., Shearman, P. L., Asner, G. P., Knapp, D. E., Aoro, G., & Lokes, B. (2013). Extreme Differences in Forest Degradation in Borneo: Comparing Practices in Sarawak, Sabah, and Brunei. *PLoS ONE*. https://doi.org/10.1371/journal.pone.0069679

Chavana-Bryant, C., Malhi, Y., Wu, J., Asner, G. P., Anastasiou, A., Enquist, B. J., et al. (2017). Leaf aging of Amazonian canopy trees as revealed by spectral and physiochemical measurements. *New Phytologist*. https://doi.org/10.1111/nph.13853

Clark, D. A. (2004). Sources or sinks? The responses of tropical forests to current and future climate and atmospheric composition. In *Philosophical Transactions of the Royal Society B: Biological Sciences*. https://doi.org/10.1098/rstb.2003.1426

da Costa, A. C. L., Galbraith, D., Almeida, S., Portela, B. T. T., da Costa, M., de Athaydes Silva Junior, J., et al. (2010). Effect of 7 yr of experimental drought on vegetation dynamics and biomass storage of an eastern Amazonian rainforest. *New Phytologist*. https://doi.org/10.1111/j.1469-8137.2010.03309.x

Curran, P. J. (1989). Remote sensing of foliar chemistry. *Remote Sensing of Environment*. https://doi.org/10.1016/0034-4257(89)90069-2

Davies, A. B., Oram, F., Ancrenaz, M., & Asner, G. P. (2019). Combining behavioural and LiDAR data to reveal relationships between canopy structure and orangutan nest site selection in disturbed forests. *Biological Conservation*. https://doi.org/10.1016/j.biocon.2019.01.032

Díaz, S., Kattge, J., Cornelissen, J. H. C., Wright, I. J., Lavorel, S., Dray, S., et al. (2016). The global spectrum of plant form and function. *Nature*. https://doi.org/10.1038/nature16489

Doughty, C. E., & Goulden, M. L. (2009a). Are tropical forests near a high temperature threshold? *Journal of Geophysical Research: Biogeosciences*. https://doi.org/10.1029/2007JG000632

Doughty, C. E., & Goulden, M. L. (2009b). Seasonal patterns of tropical forest leaf area index and CO2 exchange. *Journal of Geophysical Research: Biogeosciences*. https://doi.org/10.1029/2007JG000590

Doughty, C. E., Asner, G. P., & Martin, R. E. (2011). Predicting tropical plant physiology from leaf and canopy spectroscopy. *Oecologia*. https://doi.org/10.1007/s00442-010-1800-4

Doughty, C. E., Metcalfe, D. B., Girardin, C. A. J., Amézquita, F. F., Cabrera, D. G., Huasco, W. H., et al. (2015). Drought impact on forest carbon dynamics and fluxes in Amazonia. *Nature*. https://doi.org/10.1038/nature14213

Doughty, C. E., Santos-Andrade, P. E., Goldsmith, G. R., Blonder, B., Shenkin, A., Bentley, L. P., et al. (2017). Can Leaf Spectroscopy Predict Leaf and Forest Traits Along a Peruvian Tropical Forest Elevation Gradient? *Journal of Geophysical Research: Biogeosciences*. https://doi.org/10.1002/2017JG003883

Ewers, R. M., Didham, R. K., Fahrig, L., Ferraz, G., Hector, A., Holt, R. D., et al. (2011). A large-scale forest fragmentation experiment: The stability of altered forest ecosystems project. *Philosophical Transactions of the Royal Society B: Biological Sciences*. https://doi.org/10.1098/rstb.2011.0049

Fyllas, N. M., Quesada, C. A., & Lloyd, J. (2012). Deriving Plant Functional Types for Amazonian forests for use in vegetation dynamics models. *Perspectives in Plant Ecology, Evolution and Systematics*. https://doi.org/10.1016/j.ppees.2011.11.001

Geladi, P., & Kowalski, B. R. (1986). Partial least-squares regression: a tutorial. *Analytica Chimica Acta*. https://doi.org/10.1016/0003-2670(86)80028-9

Gvozdevaite, A., Oliveras, I., Domingues, T. F., Peprah, T., Boakye, M., Afriyie, L., et al. (2018). Leaf-level photosynthetic capacity dynamics in relation to soil and foliar nutrients along forest–savanna boundaries in Ghana and Brazil. *Tree Physiology*. https://doi.org/10.1093/treephys/tpy117

Hubau, W., Lewis, S. L., Phillips, O. L., Affum-Baffoe, K., Beeckman, H., Cuní-Sanchez, A., et al. (2020). Asynchronous carbon sink saturation in African and Amazonian tropical forests. *Nature*. https://doi.org/10.1038/s41586-020-2035-0

Jacquemoud, S., Verhoef, W., Baret, F., Bacour, C., Zarco-Tejada, P. J., Asner, G. P., et al. (2009). PROSPECT + SAIL models: A review of use for vegetation characterization. *Remote Sensing of Environment*. https://doi.org/10.1016/j.rse.2008.01.026

Krutz, D., Müller, R., Knodt, U., Günther, B., Walter, I., Sebastian, I., et al. (2019). The Instrument Design of the DLR Earth Sensing Imaging Spectrometer (DESIS). *Sensors* . https://doi.org/10.3390/s19071622

Malhi, Y., Gardner, T. A., Goldsmith, G. R., Silman, M. R., & Zelazowski, P. (2014). Tropical Forests in the Anthropocene. *Annual Review of Environment and Resources*. https://doi.org/10.1146/annurev-environ-030713-155141

Maréchaux, I., Bartlett, M. K., Sack, L., Baraloto, C., Engel, J., Joetzjer, E., & Chave, J. (2015). Drought tolerance as predicted by leaf water potential at turgor loss point varies strongly across species within an Amazonian forest. *Functional Ecology*. https://doi.org/10.1111/1365-2435.12452

McDowell, N., Allen, C. D., Anderson-Teixeira, K., Brando, P., Brienen, R., Chambers, J., et al. (2018). Drivers and mechanisms of tree mortality in moist tropical forests. *New Phytologist*. https://doi.org/10.1111/nph.15027

Meir, P., Wood, T. E., Galbraith, D. R., Brando, P. M., Da Costa, A. C. L., Rowland, L., & Ferreira, L. V. (2015). Threshold Responses to Soil Moisture Deficit by Trees and Soil in Tropical Rain Forests: Insights from Field Experiments. *BioScience*. https://doi.org/10.1093/biosci/biv107

Morton, D. C., Nagol, J., Carabajal, C. C., Rosette, J., Palace, M., Cook, B. D., et al. (2014). Amazon forests maintain consistent canopy structure and greenness during the dry season. *Nature*. https://doi.org/10.1038/nature13006

Nepstad, D. C., Tohver, I. M., David, R., Moutinho, P., & Cardinot, G. (2007). Mortality of large trees and lianas following experimental drought in an amazon forest. *Ecology*. https://doi.org/10.1890/06-1046.1

Niinemets, Ü. (2001). Global-scale climatic controls of leaf dry mass per area, density, and thickness in trees and shrubs. *Ecology*. https://doi.org/10.1890/0012-9658(2001)082[0453:GSCCOL]2.0.CO;2

Nunes, M. H., Both, S., Bongalov, B., Brelsford, C., Khoury, S., Burslem, D. F. R. P., et al. (2019). Changes in leaf functional traits of rainforest canopy trees associated with an El

Nino event in Borneo. *Environmental Research Letters*. https://doi.org/10.1088/1748-9326/ab2eae

Phillips, O. L., Aragão, L. E. O. C., Lewis, S. L., Fisher, J. B., Lloyd, J., López-González, G., et al. (2009). Drought sensitivity of the amazon rainforest. *Science*. https://doi.org/10.1126/science.1164033

Poorter, H., Niinemets, Ü., Poorter, L., Wright, I. J., & Villar, R. (2009). Causes and consequences of variation in leaf mass per area (LMA): A meta-analysis. *New Phytologist*. https://doi.org/10.1111/j.1469-8137.2009.02830.x

Poorter, L., Wright, S. J., Paz, H., Ackerly, D. D., Condit, R., Ibarra-Manríquez, G., et al. (2008). Are functional traits good predictors of demographic rates? Evidence from five neotropical forests. *Ecology*. https://doi.org/10.1890/07-0207.1

Powell, T. L., Wheeler, J. K., de Oliveira, A. A. R., da Costa, A. C. L., Saleska, S. R., Meir, P., & Moorcroft, P. R. (2017). Differences in xylem and leaf hydraulic traits explain differences in drought tolerance among mature Amazon rainforest trees. *Global Change Biology*. https://doi.org/10.1111/gcb.13731

Rifai, S. W., Girardin, C. A. J., Berenguer, E., Del Aguila-Pasquel, J., Dahlsjö, C. A. L., Doughty, C. E., et al. (2018). ENSO Drives interannual variation of forest woody growth across the tropics. *Philosophical Transactions of the Royal Society B: Biological Sciences*. https://doi.org/10.1098/rstb.2017.0410

Rifai, S. W., Li, S., & Malhi, Y. (2019). Coupling of El Niño events and long-term warming leads to pervasive climate extremes in the terrestrial tropics. *Environmental Research Letters*. https://doi.org/10.1088/1748-9326/ab402f

Riutta, T., Malhi, Y., Kho, L. K., Marthews, T. R., Huaraca Huasco, W., Khoo, M., et al. (2018). Logging disturbance shifts net primary productivity and its allocation in Bornean tropical forests. *Global Change Biology*, *24*(7), 2913–2928. https://doi.org/10.1111/gcb.14068

Rowland, L., Da Costa, A. C. L., Galbraith, D. R., Oliveira, R. S., Binks, O. J., Oliveira, A. A. R., et al. (2015). Death from drought in tropical forests is triggered by hydraulics not carbon starvation. *Nature*. https://doi.org/10.1038/nature15539

Rowland, Lucy, Lobo-do-Vale, R. L., Christoffersen, B. O., Melém, E. A., Kruijt, B., Vasconcelos, S. S., et al. (2015). After more than a decade of soil moisture deficit, tropical rainforest trees maintain photosynthetic capacity, despite increased leaf respiration. *Global Change Biology*. https://doi.org/10.1111/gcb.13035

Sala, A., Woodruff, D. R., & Meinzer, F. C. (2012). Carbon dynamics in trees: Feast or famine? *Tree Physiology*. https://doi.org/10.1093/treephys/tpr143

Saleska, S. R., Didan, K., Huete, A. R., & Da Rocha, H. R. (2007). Amazon forests green-up during 2005 drought. *Science*. https://doi.org/10.1126/science.1146663

Samanta, A., Ganguly, S., Hashimoto, H., Devadiga, S., Vermote, E., Knyazikhin, Y., et al. (2010). Amazon forests did not green-up during the 2005 drought. *Geophysical Research Letters*. https://doi.org/10.1029/2009GL042154

Serbin, S. P., Singh, A., McNeil, B. E., Kingdon, C. C., & Townsend, P. A. (2014). Spectroscopic determination of leaf morphological and biochemical traits for northern temperate and boreal tree species. *Ecological Applications*. https://doi.org/10.1890/13-2110.1

Swinfield, T., Both, S., Riutta, T., Bongalov, B., Elias, D., Majalap-Lee, N., et al. (2019). Imaging spectroscopy reveals the effects of topography and logging on the leaf chemistry of tropical forest canopy trees. *Global Change Biology*, *n/a*(n/a). https://doi.org/10.1111/gcb.14903

Thirumalai, K., DInezio, P. N., Okumura, Y., & Deser, C. (2017). Extreme temperatures in Southeast Asia caused by El Ninõ and worsened by global warming. *Nature Communications*. https://doi.org/10.1038/ncomms15531

Ustin, S. L., Asner, G. P., Gamon, J. A., Fred Huemmrich, K., Jacquemoud, S., Schaepman, M., & Zarco-Tejada, P. (2006). Retrieval of quantitative and qualitative information about plant pigment systems from high resolution spectroscopy. In *International Geoscience and Remote Sensing Symposium (IGARSS)*. https://doi.org/10.1109/IGARSS.2006.517

Ustin, S. L., Gitelson, A. A., Jacquemoud, S., Schaepman, M., Asner, G. P., Gamon, J. A., & Zarco-Tejada, P. (2009). Retrieval of foliar information about plant pigment systems from high resolution spectroscopy. *Remote Sensing of Environment*. https://doi.org/10.1016/j.rse.2008.10.019

Walsh, R. P. D., & Newbery, D. M. (1999). The ecoclimatology of Danum, Sabah, in the context of the world's rainforest regions, with particular reference to dry periods and their impact. *Philosophical Transactions of the Royal Society B: Biological Sciences*. https://doi.org/10.1098/rstb.1999.0528

Wright, I. J., Reich, P. B., Westoby, M., Ackerly, D. D., Baruch, Z., Bongers, F., et al. (2004). The worldwide leaf economics spectrum. *Nature*. https://doi.org/10.1038/nature02403

Wright, S. J., Kitajima, K., Kraft, N. J. B., Reich, P. B., Wright, I. J., Bunker, D. E., et al. (2010). Functional traits and the growth-mortality trade-off in tropical trees. *Ecology*. https://doi.org/10.1890/09-2335.1

Wu, J., Kobayashi, H., Stark, S. C., Meng, R., Guan, K., Tran, N. N., et al. (2018). Biological processes dominate seasonality of remotely sensed canopy greenness in an Amazon evergreen forest. *New Phytologist*. https://doi.org/10.1111/nph.14939

Zanne, A. E., Westoby, M., Falster, D. S., Ackerly, D. D., Loarie, S. R., Arnold, S. E. J., & Coomes, D. A. (2010). Angiosperm wood structure: Global patterns in vessel anatomy and their relation to wood density and potential conductivity. *American Journal of Botany*. https://doi.org/10.3732/ajb.0900178